Constraints on enhanced dark matter annihilation from IceCube results

Ivone F. M. Albuquerque,[1,*] Leandro J. Beraldo e Silva,[1,†] and Carlos Pérez de los Heros[2,‡]

[1]*Instituto de Física, Universidade de São Paulo, São Paulo, Brazil*
[2]*Department of Physics and Astronomy, Uppsala University, Uppsala, Sweden*

Excesses on positron and electron fluxes—measured by ATIC and the PAMELA and Fermi-LAT telescopes—can be explained by dark matter annihilation in the Galaxy, however, it requires large boosts on the dark matter annihilation rate. There are many possible enhancement mechanisms such as the Sommerfeld effect or the existence of dark matter clumps in our halo. If enhancements on the dark matter annihilation cross section are taking place, the dark matter annihilation in the core of the Earth will be enhanced. Here we use recent results from the IceCube 40-string configuration to probe generic enhancement scenarios. We present results as a function of the dark matter-proton interaction cross section, $\sigma_{\chi p}$ weighted by the branching fraction into neutrinos $f_{\nu \bar{\nu}}$ as a function of a generic boost factor B_F, which parametrizes the expected enhancement of the annihilation rate. We find that dark matter models that require annihilation enhancements of $\mathcal{O}(100)$ or more and that annihilate significantly into neutrinos are excluded as an explanation for these excesses. We also determine the boost range that can be probed by the full IceCube telescope.

I. INTRODUCTION

Several recent observations in our Galaxy have found an excess on the electron and/or positron fluxes [1–3]. However, the origin of these events is yet not clear. If they are produced according to standard physics, pulsars [4] could be the sources, as well as secondary particles created by shock accelerated hadrons inside any astrophysical source [5]. Another exciting possibility is that they may be a signature of new physics; it has been shown that dark matter annihilation in the Galaxy can describe the data [6]. However, most of these models require an enhancement on their annihilation rate. An enhancement mechanism can be found from a variety of possible phenomena such as the Sommerfeld effect, the existence of dark matter substructures in the galactic halo, or a combination of both [7,8].

Constraints on a boost factor on the dark matter annihilation rate have been recently derived from the Fermi-LAT diffuse gamma-ray measurement [9] and from their analysis of Milky Way satellite galaxies [10]. An independent and neat analysis was performed by the authors of Ref. [11], using the fact that dark matter annihilations at recombination time, redshift ~ 1000, could have injected secondary particles that could have affected the recombination processes. The measured power spectrum of the cosmic microwave background (CMB) can thus be used to set limits on the strength of the dark matter self-annihilation cross section. The IceCube collaboration has also performed an analysis searching for dark matter annihilations in the galactic halo by searching from an excess diffuse neutrino flux over the expected atmospheric flux [12]. The results can also be used to set limits on a boost in the annihilation cross section.

These methods show some degree of complementarity since each one provides better sensitivity to a different range of the mass of the dark matter particles or to different annihilation channels. They also rest on different assumptions and approximations. Fermi and the CMB method are competitive in the low mass range (dark matter massed ≲ 1 TeV), while the IceCube analysis reaches 10 TeV and can also probe annihilation directly into neutrinos. There is some halo-model dependency when setting limits on the annihilation cross section from the observations of satellite galaxies: the expected signal depends on the degree of cuspiness of the assumed halo. On the other hand, the CMB analysis does not depend on the shape of dark matter haloes since there are no gravitationally bound structures at the redshift considered, but it depends on assumptions about the fraction of the energy released by the annihilating dark matter particles and how it is absorbed by the surrounding medium.

In this paper we follow the alternative approach proposed in Ref. [13]. The authors argue that an enhancement of the dark matter annihilation rate should also boost the neutrino flux from dark matter annihilations in the center of the Earth. A thermal annihilation cross section implies that dark matter capture and annihilation has not yet reached equilibrium in the Earth. However, it is not necessary that the annihilation cross section has to remain the same as during the freeze-out period. If the annihilation rate is somehow enhanced in the post freeze-out period, the equilibrium might already have been achieved. In the next section we will show that the annihilation rate reaches its

*ifreire@if.usp.br
†lberaldo@if.usp.br
‡cph@physics.uu.se

maximum at the equilibrium and then depends only in the capture rate. A boost in the annihilation rate increases the flux of annihilation products until it reaches its maximum. In this case the neutrino flux from the center of the Earth will be large enough to be detected by telescopes such as IceCube. In short, if the dark matter annihilation rate is enhanced, the time scale for equilibrium diminishes. Consequently the flux of annihilation products is expected to be at or closer to its peak value. Therefore much larger than the resulting flux from when the capture and annihilation rate are far from equilibrium.

We use the recently published IceCube results on a search for a diffuse flux of muon neutrinos [14] to set limits on a boost factor in the dark matter annihilation cross section. IceCube has measured neutrinos coming from near or below the horizon in the energy range 332 GeV and 84 TeV using data taken with the 40-string detector configuration (IceCube-40). The analysis includes all events coming from near or below the horizon, and the result is compatible with the expected atmospheric neutrino flux (see also Ref. [15]). It is also generic enough to allow comparison with our prediction of the flux of muon neutrinos produced in dark matter annihilations in the center of the Earth. We determine this flux by simulating the annihilation of WIMP-type particles in the center of the Earth and propagating the neutrinos to the detector. A significant neutrino flux from dark matter annihilation should be seen above the expected atmospheric neutrino flux. If not, limits can be set on the model used to determine the dark matter signal. Our analysis shows that models which require very large boosts on the dark matter annihilation rate in order to explain the excess seen in the galactic positron and electron flux and have an annihilation channel into neutrinos are ruled out.

In Sec. II we describe dark matter capture and annihilation in the Earth. In Secs III and IV we describe the signal simulation and calculate the expected number of events in the IceCube-40 detector. We then compare our results with the IceCube-40 published results, showing the boost factor range that is excluded. Finally, in Sec. V we estimate the sensitivity region for the full 86-string detector.

II. DARK MATTER ANNIHILATION IN THE EARTH

Dark matter interactions in the Earth will be dominated by spin-independent elastic scattering since the most abundant isotopes of the Earth's core and mantle are spin-0 nuclei. The time evolution of the number of dark matter particles will result from a balance between the capture (Γ_C) and annihilation rate (Γ_A),

$$\dot{N} = \Gamma_C - 2\Gamma_A. \qquad (1)$$

The Earth's dark matter capture rate is given by [13,16]

$$\Gamma_C \simeq 9.6 \times 10^{11} \frac{\rho_\chi}{0.3 \text{ GeV/cm}^3} \left(\frac{270 \text{ km/s}}{v_\chi}\right)^3 \left(\frac{\text{TeV}}{m_\chi}\right)^2$$

$$\times \left(\frac{\sigma_{\chi p}}{10^{-42} \text{ cm}^2}\right) \text{ s}^{-1}, \qquad (2)$$

here $\sigma_{\chi p}$ is the spin-independent dark matter cross section off protons, v_χ and ρ_χ are the dark matter velocity and density in the halo, and m_χ is the dark matter particle mass. In deriving the above equation it is assumed that for masses m_χ much larger than the nucleus mass, the dark matter interaction cross section off a proton is the same as off a neutron. In this case, the spin-independent cross section off a nucleus with mass number A is given by $\sigma_{\chi N} \sim A^4 \sigma_{\chi p}(1 - 2m_p/m_\chi)$, where m_p is the proton mass.

The annihilation rate depends both on the relative velocity-scaled cross section $\langle \sigma_A v \rangle$ as well as on the dark matter distribution in the Earth [17]. The latter can be given in terms of the parameter $C_A \equiv \langle \sigma_A v \rangle / V_{\text{eff}}$, where $\Gamma_A = N^2 C_A/2$, and $V_{\text{eff}} = 5.7 \times 10^{22} (\text{TeV}/m_\chi)^{3/2}$ cm^3 represents the dark matter effective volume in the core of the Earth, assuming an isothermal distribution [16,18].

The solution to the dark matter time evolution in the Earth [Eq. (1)] is then,

$$\Gamma_A = \frac{\Gamma_C}{2} \tanh^2\left(\frac{t_\oplus}{\tau}\right), \qquad (3)$$

where $t_\oplus$ is the age of the solar system and $\tau = 1/\sqrt{\Gamma_c C_A}$ is the time scale for equilibrium between capture and annihilation. An enhancement on the annihilation rate will only be effective if it can accelerate equilibrium within the Earth. When the equilibrium stage is reached, the annihilation is maximum and depends entirely on the capture rate ($\Gamma_A = \Gamma_C/2$). Thermal relic dark matter candidates typically have $\langle \sigma_A v \rangle_r = 3 \times 10^{-26}$ cm^3 s^{-1}, which makes $C_{Ar} \simeq 5.3 \times 10^{-49} (m_\chi/\text{TeV})^{3/2}$ s^{-1}, and for these values the Earth is today far from equilibrium.

In our analysis we consider scenarios where the annihilation cross section is enhanced by boosting the thermal relic annihilation rate Γ_{Ar} by a generic factor B_f, which affects the nonequilibrium rate through $C_A = B_f C_{Ar}$. Such parametrization, though adequate to probe enhancements due to Sommerfeld effect or to new interaction mechanisms, cannot probe enhancements due to a possible dark matter halo substructure. In this latter case, a standard annihilation cross section could well account for any possible signal, which would be due to the increased local dark matter density and not due to any new feature of the annihilation process itself.

III. NEUTRINO PRODUCTION

The escape velocity at the Earth's core is $v_e \approx 15$ km/s and dark matter moves very slowly inside the Earth. The annihilation products will, therefore, be monochromatic

and produced with the same energy as the dark matter mass. Here we consider the annihilation into a muon-neutrino pair (which we call primary neutrinos). "Secondary" neutrinos are also produced in the decay of other primary annihilation particles such as τ's, t's, W's, and b's. Since the explanation of the observed leptonic excess in terms of dark matter also has to account for the fact that no antiproton excess was found by PAMELA [19], annihilation into leptons is preferred when compared to hadrons. Secondary neutrinos from annihilation into charged lepton states, specifically on $\tau\bar{\tau}$, were analyzed in Ref. [13]. The energies of these secondary neutrinos will be spread at relatively low values (~ 50 GeV) compared to the primary neutrino flux and detection in neutrino telescopes is then disfavored (unreasonably large boost factors would be needed to bring such flux over the atmospheric neutrino background to a detectable level). We will, therefore, not take into account the secondary neutrino flux in our calculations and instead concentrate on the easily detectable monochromatic flux from direct annihilations.

The primary neutrino flux produced from dark matter annihilations in the Earth's center is given by

$$\frac{d\phi_\nu}{dE_\nu dAdtd\Omega} = \frac{f_{\nu\bar{\nu}}\Gamma_A}{4\pi R_\oplus^2}\frac{dN_\nu}{dE_\nu}, \tag{4}$$

where $f_{\nu\bar{\nu}}$ is the annihilation branching ratio into $\nu_\mu\bar{\nu}_\mu$, $R_\oplus$ is the radius of the Earth, and dN_ν/dE_ν is the energy distribution of the neutrinos produced in the annihilations. We show our results for two generic cases, $m_\chi = 500$ GeV and $m_\chi = 1000$ GeV, which are representative of the models that fit the observed positron and electron excess and then later on for $m_\chi = 5000$ GeV when comparing our results to others. Since at these energies neutrinos practically do not lose energy on their way from the center of the Earth to the detector, the term dN_ν/dE_ν will be a delta function at the dark matter masses considered.

IV. CONSTRAINTS ON THE ANNIHILATION BOOST FACTOR FROM ICECUBE-40

In order to predict the muon flux from dark matter annihilation in the Earth at the IceCube detector in the South Pole, we use the publicly available WIMPSIM code [20]. We simulate a monochromatic muon-neutrino beam at the center of the Earth, with energy equal to the dark matter mass, by selecting the muon-neutrino channel. WIMPSIM simulates the propagation of these neutrinos, including energy losses and charged and neutral current interactions, as well as, oscillations through the Earth. The muon-neutrino flux at the detector is given as an output. Although we have chosen to simulate the flux specifically for the location of the IceCube detector, the detector site is not relevant in this case and the results and sensitivities presented in the next sections can easily be interpreted for any neutrino telescope of similar size.

The number of muons from dark matter annihilation from a given angular region Ω and during an exposure t_{exp} in IceCube-40 is then

$$N_\mu = \int \frac{d\phi_\nu}{dE_\nu dAdtd\Omega} dE_\nu t_{\mathrm{exp}} A_{\mathrm{eff}}\Omega. \tag{5}$$

We proceed then by convoluting the muon-neutrino flux with the IceCube-40 effective area published in Ref. [14]. The effective area accounts for the detector efficiency including the neutrino-nucleon interaction probability, the muon energy loss from its production point to the detector, and the detector trigger, and analysis efficiency. As the neutrino beam is monochromatic, we use the corresponding value of A_{eff} for each dark matter mass considered. The muon-neutrino angular distribution is the main parameter for background reduction in our analysis. Figure 1 shows the angular distribution from neutrinos from dark matter annihilation in the center of the Earth. It is collimated in a angle of less than approximately 3° around the vertical direction $\theta = 180°$. This figure also shows the smearing effect due to the angular resolution of the detector, taken here conservatively to be 2° for up-going vertical events. Therefore, we use the effective area for the zenith range $150° < \theta < 180°$ from Ref. [14]. Even though such angular range is much wider than that from the expected signal, the
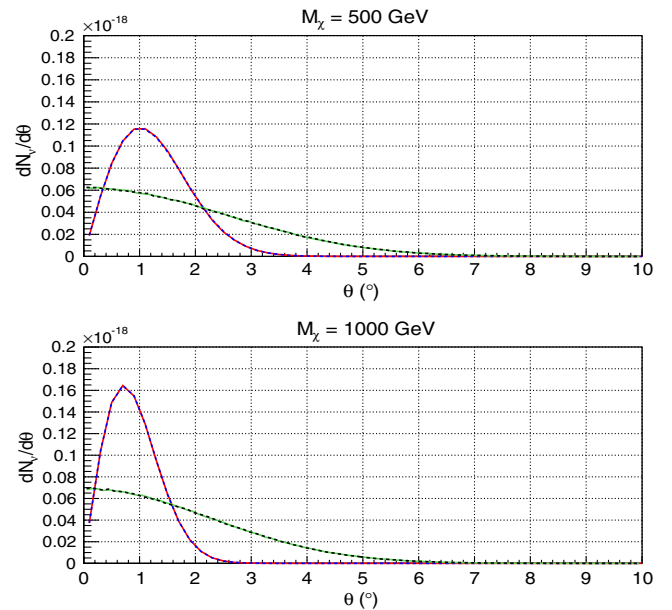

FIG. 1 (color online). Angular distributions of the primary muon-neutrino and antineutrino flux from dark matter annihilations at the center of the Earth with respect to the vertical direction (pink lines). The green curves show the angular distribution smeared by the detector angular resolution, taken as 2°. The bottom plot shows the distribution for 1 TeV dark matter, while the plot on the top for 500 GeV dark matter. Full lines are for neutrinos and dashed lines are for antineutrinos.

effective area does not vary considerably with zenith angle below about 10 TeV, where Earth absorption effects start to be important.

For our analysis, we choose an angular window from the vertical direction that contains 90% of the expected signal (4.1°(3.7°) for 500(1000) GeV dark matter, respectively, where the angular experimental resolution has been taken into account) and use the calculated number of events with Eq. (5) as the signal. We have not used any energy information in this analysis, using only the total number of events predicted and detected to derive our exclusion regions. We will, however, present a study on the effect of the detector energy resolution in the sensitivity study for the complete IceCube detector in the next section. Figure 2 shows the predicted number of $\nu_\mu + \bar{\nu}_\mu$ in IceCube-40 with $t_{\text{exp}} = 375.5$ days as a function of the dark matter nucleon cross section $\sigma_{\chi p}$ scaled by the branching ratio for different boosts factors. As shown, larger enhancements on the annihilation rate result in a shorter time for equilibrium among capture and annihilation.

In order to study the model rejection power of our analysis in a quantitative way, we determine the statistical significance of the predicted dark matter signal $S/\sqrt{B}$ as a function of boost factor, where S is the number of signal events predicted in the given angular cone. As the background B, we use the measured number of events in IceCube-40 in the same angular regions.

Two recent IceCube publications, a measurement of the atmospheric neutrino flux [15], and a search for a diffuse E^{-2} flux of cosmic origin [14] give results that are consistent with the expected atmospheric neutrino flux. We use the publicly available data from the diffuse analysis, which is available at Ref. [21]. This analysis selects events coming from near or below the horizon. The background is composed of atmospheric muons arriving from above the detector and misreconstructed as an event coming from below. The rejection of these events is described in Ref. [14] and the background contamination in the data sample is estimated to be less than 1%. The final data sample contains 13K events and it is given as a function of the zenith angle. This allows us to select events which come in the same direction as expected signal dark matter annihilations. The data is then reduced to 14 (9) events when considering the angular regions expected for 500(1000) GeV dark matter neutrinos. We compare this number to the predicted number of events from our signal choices and for different boost factors.

The result is presented in Fig. 3, which shows the boost factor versus $\sigma_{\chi p}$ scaled by the $\nu\bar{\nu}$ branching ratio region, which was probed in this analysis. The plot to the left is for 500 GeV dark matter and the one to the right is for 1 TeV. The light-green, solid line shows a 5σ exclusion; above this line the exclusion is more strict according to the color-coded bar on the right side. This bar indicates the level of statistical significance. The best limit on $\sigma_{\chi p}$ comes from the Xenon100 collaboration [22]. At 90% C.L. 500 GeV dark matter models are constrained above $\sigma_{\chi p} \approx 4 \times 10^{-44}$ cm^2 and 1 TeV dark matter above $\sigma_{\chi p} \approx 8 \times 10^{-44}$ cm^2. We draw this limit on Fig. 3 as a reference since direct detection results do not depend on $f_{\nu\bar{\nu}}$ neither on any boost factor. For such a limit, boost factors above 215 and 58, respectively, are excluded at a 5σ level. This exclusion requires, however, that $f_{\nu\bar{\nu}} = 1$, i.e., annihilation exclusively into neutrinos, which may be difficult to justify phenomenologically. It should be noted that the excluded region in Fig. 3 does not require necessarily a 100% annihilation into neutrinos. One can lower the branching factor by increasing the required boost factor limit. As one moves down along the green 5σ-limit line, larger boost factors are disfavored as the quantity $\sigma_{\chi p} \times f_{\nu\bar{\nu}}$ becomes lower. Lower values of $\sigma_{\chi p} \times f_{\nu\bar{\nu}}$ can be achieved either by models with relatively high cross sections but lower branching ratio to neutrinos or by lower cross sections with higher annihilation probability to neutrinos. In either case, the expected signal in IceCube would decrease and a higher boost factor would be needed to bring it to the current sensitivity of the detector. Higher boost factors to the right of the green line would then be disfavored at a higher significance.

The degeneracy of the product $\sigma_{\chi p} \times f_{\nu\bar{\nu}}$ can be broken when considering specific dark matter models with known branching ratio to neutrinos and cross section with protons. Figure 3 can then be used to determine the minimum boost factor which is disfavored at a 5σ level.
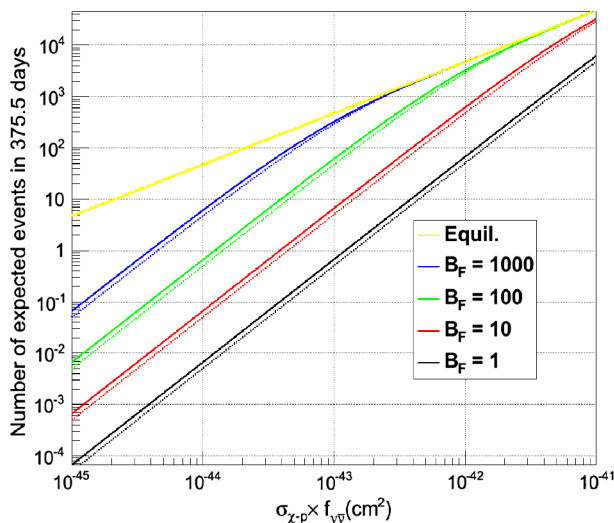

FIG. 2 (color online). Predicted number of $\nu_\mu + \bar{\nu}_\mu$ from dark matter annihilation in the Earth at IceCube-40. Results are for 375.5 days of exposure for different boost factor values (color coded as labeled). Dashed lines are for 1 TeV and solid lines for 500 GeV dark matter.
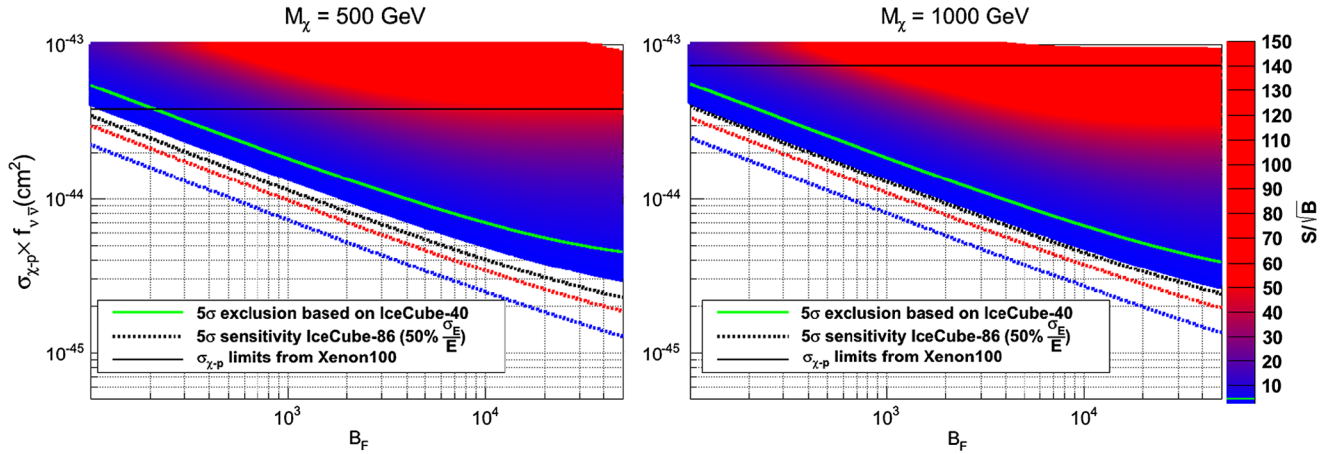
FIG. 3 (color online). Boost factor versus dark matter nucleon interaction cross section $\sigma_{\chi p}$ scaled by $\nu\bar{\nu}$ branching ratio ($f_{\nu\bar{\nu}}$). The light-green, solid line indicates the exclusion at 5σ level based on our analysis of IceCube-40 results. Above this line the exclusion is more strict accordingly to the color-coded bar at the side. The color coded bar represents the statistical significance level ($S/\sqrt{B}$). Both the bar as well as the contour in this figure start at 3σ. The black, (red, blue) dashed line is the 5σ sensitivity for the IceCube-86 telescope with 50% (30%, 10%)% energy resolution. As a reference, the black, solid lines represent the 90% C.L. constraints on $\sigma_{\chi p}$ from direct detection [22] (independent of the boost factor and of the annihilation branching ratio $f_{\nu\bar{\nu}}$). The plot to the left is for 500 GeV dark matter and the one to the right for 1000 GeV.

V. PREDICTION FOR FULL ICECUBE DETECTOR

The full IceCube detector with 86 strings (IceCube-86) is now completed and has been taking data since May 2011. In order to estimate the full detector sensitivity, we can use the fact that the atmospheric neutrino flux measured by IceCube-40 [14,15] is consistent with model expectations as, for example, the one proposed by Ref. [23]. We will also go one step further than the calculations in Sec.IV and assume that IceCube will be able to estimate the neutrino energy with a given resolution σ_E. We assume three benchmark energy resolutions, $\sigma_E = 0.1E$, $0.3E$, and $0.5E$ which go from the very optimistic to the more conservative situation in a neutrino telescope. The 40-string configuration has its energy resolution between 50% and 80%. We assume here that the complete detector can reach a better resolution in any case. We note that energy estimation in neutrino telescopes is a difficult task since muon tracks above a few 100 GeV will cross the detector volume, and the neutrino energy can only be estimated through model-dependent deconvolution methods.

An effective area at trigger level for the complete IceCube-86 detector has been published in Ref. [24]. However, the effective area at final analysis level can differ significantly from trigger level, since data quality cuts are applied to the data sample to reduce background but also inevitably reduce signal efficiency. In practice, one can just rescale the IceCube-40 effective area by 2.15 (which scales 40 to 86 strings) since at the energies considered in our analysis, and for vertical events, each string is

practically an independent detector and, therefore, in a first approximation the effective area scales proportionally to just the number of strings. We expect, though, that a dedicated analysis with IceCube-86 to be more efficient at lower energies than the IceCube-40 analysis we have used in the previous section; since we will be integrating $A_{\text{eff}} \times$ flux in a range of energies, we need to be careful with the behavior of the effective area with energy. We have, therefore, normalized the IceCube-86 effective area from Ref. [24] with the rescaled IceCube-40 area at 10 TeV, where the IceCube-40 analysis is optimal. The shape of the IceCube-86 effective area at lower energies automatically takes into account the improved capabilities of the full detector at energies below 1 TeV.

We now have all ingredients we need to estimate the sensitivity of the IceCube-86 detector. We calculate the number of atmospheric neutrino events from within a vertical cone of 4.1° and 3.7° aperture by convoluting the detector effective area with the parametrization of the atmospheric neutrino flux taken from Ref. [23]. Instead of choosing a delta function for the spectrum as in the previous case, we introduce a smearing in the energy according to the assumed energy resolution. In practice, this translates into that we perform the $A_{\text{eff}} \times$ flux integral between $m_\chi - \sigma_E$ and $m_\chi + \sigma_E$. We assume that the measurement of IceCube will be compatible with the calculated number of background events and calculate the sensitivity to an excess neutrino flux from the center of the Earth under this assumption. The result of this exercise is shown in Fig. 3. The black (red, blue) dashed lines in both plots represent 5σ sensitivity

that can be achieved in 1 yr live time of IceCube-86 ($t_{\exp 86} = 365$ d) assuming a 50% (30% ,10)% energy resolution.

VI. CONCLUSIONS

If dark matter annihilation in our Galaxy is responsible for the excesses seen by ATIC [1], PAMELA [2], and Fermi-LAT [3], an enhancement on the dark matter annihilation rate in the Earth should also be foreseen. This enhancement might bring the equilibrium among the dark matter capture and annihilation rates to occur much earlier than the time scale expected from a purely thermal annihilation rate. In this case, the neutrino flux from dark matter captured in the Earth can be quite large. We present results as a function of the dark matter-proton interaction cross section $\sigma_{\chi p}$ weighted by the branching fraction into neutrinos $f_{\nu\bar{\nu}}$ as a function of a generic boost factor B_F, which parametrizes the expected enhancement of the annihilation rate. In this sense, it is important to note that our results do not depend on the details of the mechanism which enhances the annihilation cross section. We have used two benchmark models, a 500 GeV and 1 TeV generic WIMP annihilating in the center of the Earth to scan the ($\sigma_{\chi p} \times f_{\nu\bar{\nu}}$, B_F) parameter space and set constrains on this two-dimensional space using current IceCube results. Our calculations assume that the dark matter velocity distribution is Gaussian as well as that dark matter collected in the Earth's core follows an isothermal distribution.

In order to explain the positron and electron excesses that are seen, models also have to cope with the fact that the antiproton spectrum measured by PAMELA [19] is in full agreement with the expectation from secondary production of antiprotons from propagation of cosmic rays in the Galaxy. This rules out as an explanation of the excess many dark matter models with preferred annihilation into heavy products, producing many antiprotons. Therefore, leptophilic models, which propose dark matter annihilation exclusively into leptons, are favored as an explanation to the excesses found. We have shown that when 500(1000) GeV dark matter annihilates into a large fraction of neutrinos, annihilation boost factors of the $\mathcal{O}(100)$ and above are already constrained by our analysis at a 5σ level or higher, depending on the interaction cross section assumed. Thus, leptophilic models [25] which favor primary neutrino production are constrained by our results.

In order to compare this analysis to others, we show in Fig. 4 limits on $\langle\sigma_A \times \upsilon\rangle$ as a function of m_χ from Fermi [10], CMB [11], and IceCube [26]. Our bounds as a function of $\langle\sigma_A \times \upsilon\rangle$ can be determined from Eq. (4). It can also easily be visualized in Fig. 3, where a 3σ significance is shown as the edge of the shaded area: the limit on the annihilation cross section is determined from each boost factor value on this curve. In Fig. 4 these are shown for
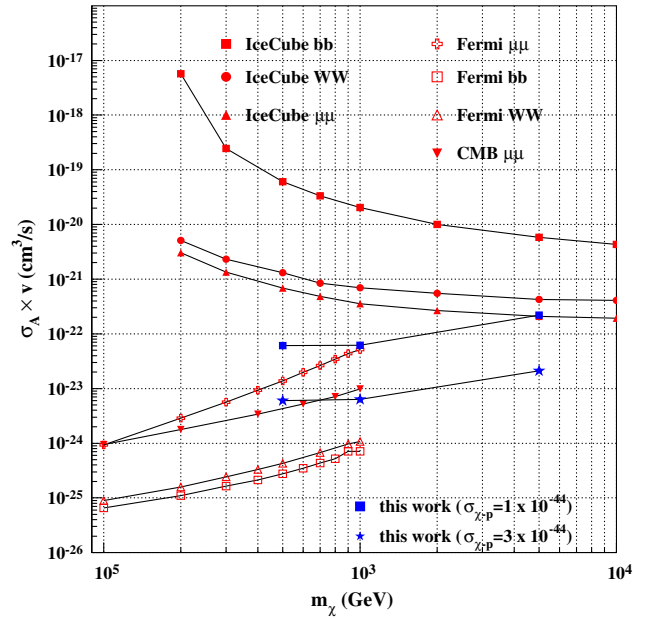

FIG. 4 (color online).   Bounds on the dark matter annihilation cross section σ_A versus mass m_χ by Fermi [10], IceCube [26], analysis over CMB data [11] and this work, where two different $\sigma_{\chi p}$ values of 3×10^{-44} cm^2 (blue star) and 1×10^{-44} cm^2 (blue, solid square) are assumed. Here we also plot our results assuming a 5 TeV dark matter mass. Our limits correspond to a 3σ significance level, while the others are at 90% C.L.

two choices of $\sigma_{\chi p}$, 3×10^{-44} cm^2 (blue stars), and 1×10^{-44} cm^2 (blue, solid squares), which are below the current Xenon limit [22].

Our results and IceCube's are the only ones to probe annihilation into neutrinos. Other limits coming from searches with gammas from satellite galaxies by Fermi [10] or from the analysis based on the CMB [11] imprint at high redshifts are complementary since they probe different annihilation channels and also rest on different underlying assumptions.

We also investigated the reach of the completed IceCube 86-string detector, and we presented results of its sensitivity in the ($\sigma_{\chi p} \times f_{\nu\bar{\nu}}$, B_F) parameter space. We have estimated how using neutrino energy information could improve the analysis, and in Fig. 3 we showed the expected sensitivity for three different assumptions of the detector energy resolution.

ACKNOWLEDGMENTS

[1] J. Chang *et al.*, Nature (London) **456**, 362 (2008).

[2] Astropart. Phys. **34**, 1 (2010); O. Adriani *et al.* (PAMELA Collaboration), Phys. Rev. Lett. **102**, 051101 (2009).

[3] A. A. Abdo *et al.* (Fermi-LAT Collaboration), Phys. Rev. Lett. **102**, 1811101 (2009).

[4] S. Profumo, Central Eur. J. Phys. **10**, 1 (2011).

[5] P. Blasi, Phys. Rev. Lett. **103**, 051104 (2009).

[6] M. Cirelli and A. Strumia, Proc. Sci., IDM2008 (2008) 089 [arXiv:0808.3867]; I. Cholis, L. Goodenough, D. Hooper, M. Simet, and N. Weiner, Phys. Rev. D **80**, 123511 (2009); D. P. Finkbeiner, L. Goodenough, T. R. Slatyer, M. Vogelsberger, and N. Weiner, J. Cosmol. Astropart. Phys. 05 (2011) 002.

[7] I. Cholis and L. Goodenough, J. Cosmol. Astropart. Phys. 09 (2010) 010.

[8] M. Lattanzi and J. Silk, Phys. Rev. D **79**, 083523 (2009).

[9] A. A. Abdo *et al.* (Fermi-LAT Collaboration), J. Cosmol. Astropart. Phys. 04 (2010) 014.

[10] A. Ackermann *et al.* (Fermi-LAT Collaboration), Phys. Rev. Lett. **107**, 241302 (2011).

[11] S. Galli, F. Iocco, G. Bertone, and A. Melchiorri, Phys. Rev. D **84**, 027302 (2011); G. Hütsi, J. Chluba, A. Hektor, and M. Raidal, Astron. Astrophys. **535**, A26 (2011).

[12] R. Abbasi *et al.* (IceCube Collaboration), Phys. Rev. D**84**, 022004 (2011).

[13] C. Delaunay, P. J. Fox, and G. Perez, J. High Energy Phys. 05 (2009) 099.

[14] R. Abbasi *et al.* (IceCube Collaboration), Phys. Rev. D **84**, 082001 (2011).

[15] R. Abbasi *et al.* (IceCube Collaboration), Phys. Rev. D **83**, 012001 (2011).

[16] G. Jungman, M. Kamionkowski, and K. Griest, Phys. Rep. **267**, 195 (1996).

[17] K. Griest and D. Seckel, Nucl. Phys. **B283**, 681 (1987).

[18] A. Gould, Astrophys. J. **321**, 571 (1987).

[19] O. Adriani *et al.*, (PAMELA Collaboration), Phys. Rev. Lett. **105**, 121101 (2010).

[20] M. Blennow, J. Edsjö, and T. Ohlsson, J. Cosmol. Astropart. Phys. 01 (2008) 021.

[21] http://www.icecube.wisc.edu/science/data/.

[22] E. Aprile *et al.* (XENON100 Collaboration), Phys. Rev. Lett. **107**, 131302 (2011).

[23] M. Honda, T. Kajita, K. Kasahara, S. Midorikawa, and T. Sanuki, Phys. Rev. D **75**, 043006 (2007).

[24] C. Wiebusch, (IceCube Collaboration), arXiv:0907.2263v1.

[25] P. J. Fox and E. Poppitz, Phys. Rev. D **79**, 083528 (2009).

[26] R. Abbasi *et al.* (IceCube Collaboration), Phys. Rev. D **84**, 022004 (2011); (IceCube Collaboration), arXiv:1111.2738.